THE JOURNAL OF BIOLOGICAL CHEMISTRY VOL. 283, NO. 3, pp. 1525–1533, January 18, 2008

Site-specific Incorporation of Keto Amino Acids into Functional G Protein-coupled Receptors Using Unnatural Amino Acid Mutagenesis*[S]

Received for publication, August 31, 2007, and in revised form, November 7, 2007 Published, JBC Papers in Press, November 8, 2007, DOI 10.1074/jbc.M707355200

Shixin Ye[‡1,2], Caroline Köhrer[§1], Thomas Huber[‡], Manija Kazmi[‡], Pallavi Sachdev[‡3], Elsa C.Y. Yan[‡4], Aditi Bhagat[‡4], Uttam L. RajBhandary[§5], and Thomas P. Sakmar[‡6]

From the [‡]Laboratory of Molecular Biology and Biochemistry, The Rockefeller University, New York, New York 10065, and the [§]Department of Biology, Massachusetts Institute of Technology, Cambridge, Massachusetts 02139

G protein-coupled receptors (GPCRs) are ubiquitous heptahelical transmembrane proteins involved in a wide variety of signaling pathways. The work described here on application of unnatural amino acid mutagenesis to two GPCRs, the chemokine receptor CCR5 (a major co-receptor for the human immunodeficiency virus) and rhodopsin (the visual photoreceptor), adds a new dimension to studies of GPCRs. We incorporated the unnatural amino acids *p*-acetyl-L-phenylalanine (Acp) and *p*-benzoyl-L-phenylalanine (Bzp) into CCR5 at high efficiency in mammalian cells to produce functional receptors harboring reactive keto groups at three specific positions. We obtained functional mutant CCR5, at levels up to ~50% of wild type as judged by immunoblotting, cell surface expression, and ligand-dependent calcium flux. Rhodopsin containing Acp at three different sites was also purified in high yield (0.5–2 μg/10^7 cells) and reacted with fluorescein hydrazide *in vitro* to produce fluorescently labeled rhodopsin. The incorporation of reactive keto groups such as Acp or Bzp into GPCRs allows their reaction with different reagents to introduce a variety of spectroscopic and other probes. Bzp also provides the possibility of photo-cross-linking to identify precise sites of protein-protein interactions, including GPCR binding to G proteins and arrestins, and for understanding the molecular basis of ligand recognition by chemokine receptors.

Seven-transmembrane helical G protein-coupled receptors (GPCRs)[7] comprise a superfamily of cell surface proteins that participate in the most important and diverse signaling pathways in nature (1). The human genome encodes ~725 such receptors, and mutations in them cause a variety of diseases. GPCRs are, therefore, the target of a large fraction of drugs on the market (2, 3). Activation of GPCRs requires the binding of a ligand. Understanding the molecular mechanism of ligand recognition, GPCR activation, and subsequent receptor interaction with G proteins is an important goal in studies of GPCRs. The most informative model system to date has been the visual pigment, rhodopsin (activated by light), which is especially well suited for various spectroscopic studies that can be interpreted in the context of high resolution crystal structures (4–6).

Current dynamic studies of other GPCRs rely on fluorescence techniques. However, methods currently available for dynamic studies of fluorescently labeled GPCRs in reconstituted model systems have inherent limitations. The two most common methods to introduce site-specific fluorescent labels, maleimide chemistry targeting cysteine residues and the use of green fluorescent protein fusions, are cases in point. The former method requires either detailed exploration of labeling conditions to control the precise labeling site with wild-type receptors in the native membrane environment (7), or replacement of naturally occurring cysteines with unreactive amino acids by site-directed mutagenesis (6, 8). One obvious technical problem with the mutagenesis approach is that the substitution of multiple cysteines in a GPCR might have unintended or unforeseen effects on function. Green fluorescent protein fusions provide technical convenience and have been mostly used for cell-based studies of trafficking, subcellular localization, and receptor dimerization. A disadvantage of this method is the size of the green fluorescent protein fusion tag (238 amino acids with a molecular mass of ~30 kDa), which might interfere with the GPCR function or reconstitution. Single-molecule fluorescence resonance energy transfer, or related ensemble methods, is potentially the most promising tool to study con-

* This work was supported in part by the Ellison Medical Foundation and the Allene Reuss Memorial Trust (to T. P. S.) and by National Institutes of Health Grant GM67741 and U.S. Army Research Office Grant W911NF-04-1-0353 (to U. L. R.). The costs of publication of this article were defrayed in part by the payment of page charges. This article must therefore be hereby marked "*advertisement*" in accordance with 18 U.S.C. Section 1734 solely to indicate this fact.

[S] The on-line version of this article (available at http://www.jbc.org) contains supplemental Figs. S1–S3 and Tables S1 and S2.

[1] Both authors contributed equally to this work.

[2] Supported by a C.H. Li Fellowship of The Rockefeller University.

[3] A Murray Foundation fellow.

[4] Current address: Dept. of Chemistry, Yale University, New Haven, CT 06520.

[5] To whom correspondence may be addressed: Dept. of Biology, Massachusetts Institute of Technology, 77 Massachusetts Ave., Cambridge, MA 02139. Tel.: 617-253-4702; Fax: 617-252-1556; E-mail: bhandary@mit.edu.

[6] To whom correspondence may be addressed: Laboratory of Molecular Biology and Biochemistry, The Rockefeller University, 1230 York Ave., New York, NY 10065. Tel.: 212-327-8288; Fax: 212-327-7904; E-mail: sakmar@rockefeller.edu.

[7] The abbreviations used are: GPCR, G protein-coupled receptor; aaRS, aminoacyl-tRNA synthetase; TyrRS, tyrosyl-tRNA synthetase; AcpRS, *p*-acetyl-L-phenylalanyl-tRNA synthetase; BzpRS, *p*-benzoyl-L-phenylalanyl-tRNA synthetase; Acp, *p*-acetyl-L-phenylalanine; Bzp, *p*-benzoyl-L-phenylalanine; *Bst*-Yam, amber suppressor tRNA derived from *B. stearothermophilus* tRNA^{Tyr}; FLuc, firefly luciferase; aa, amino acid(s); rho, rhodopsin; wt, wild type; RANTES, regulated on activation normal T cell expressed and secreted; DM, *n*-dodecyl-β-D-maltoside.

formational dynamics and structure. However, such studies are not generally feasible for GPCRs, because they require specific labeling of receptors at very high yield, generally with suitable donor and acceptor fluorophore pairs. Clearly, the development of an alternative and efficient site-specific labeling technique would greatly facilitate dynamic studies of receptors. This challenge prompted us to introduce specific reactive amino acid side chains, suitable for further derivatization with a wide variety of fluorescent tags, into GPCRs while leaving their cellular biogenesis and function intact.

An important recent advance biology has been the development of unnatural amino acid mutagenesis involving readthrough of an amber (UAG) codon in an mRNA by a suppressor tRNA aminoacylated with the unnatural amino acid. Unnatural amino acids with novel chemical, physical, and biological properties have been incorporated into proteins in prokaryotic and eukaryotic systems (9–22). Two different approaches are used for the synthesis of the aminoacylated suppressor tRNAs: (i) chemical aminoacylation of suppressor tRNAs and (ii) introduction of engineered aminoacyl-tRNA synthetase (aaRS)/suppressor tRNA pairs that aminoacylate the suppressor tRNA *in vivo* with the desired unnatural amino acid. The chemical approach (23) is more versatile and allows the attachment of virtually any unnatural amino acid of interest to the suppressor tRNA. Dougherty and co-workers (17, 24, 25) adapted this approach successfully to studies of ion channels, γ-aminobutyric acid and nicotinic receptors expressed in *Xenopus* oocytes. Highly sensitive measurements of unique channel activities made the absolute expression yield non-critical, with single cell expression being sufficient. However, these and other studies (26) have been mostly limited to oocytes. The low yield and the technical difficulties to produce and deliver chemically aminoacylated suppressor tRNA into a large number of mammalian cells made this method impractical for general studies of GPCRs. In recent years, the alternative approach involving aaRS/suppressor tRNA pairs has opened up the possibility for synthesis *in vivo* of functionally active proteins containing unnatural amino acids, thereby providing a promising approach to study GPCRs using simplified procedures that any typical biochemistry or biophysics laboratory can undertake.

High level site-specific incorporation of unnatural amino acids into proteins requires first the availability of orthogonal aaRS/suppressor tRNA pairs (27–29). These aaRSs are then mutagenized and used for generating suppressor tRNAs aminoacylated with the unnatural amino acid of choice *in vivo*. An orthogonal pair consisting of an amber suppressor tRNA derived from *Bacillus stearothermophilus* $tRNA^{Tyr}$ (*Bst*-Yam) and mutants derived from *Escherichia coli* tyrosyl-tRNA synthetase (TyrRS) (Y37V/Q195C) was first established in mammalian cells for incorporation of 3-iodo-L-tyrosine into reporter proteins such as Ras, epidermal growth factor receptor, and cyan fluorescent protein (16). Schultz and co-workers evolved several variants of *E. coli* TyrRS using positive and negative selections in *Saccharomyces cerevisiae* (18) for the incorporation of other unnatural amino acids, including *p*-acetyl-L-phenylalanine (Acp) and *p*-benzoyl-L-phenylalanine (Bzp). More recently, the combination of *Bst*-Yam with one of these TyrRS variants (Y37G/D182G/L186A) was used to successfully incorporate Bzp into Grb2 protein in mammalian cells (21).

For this study, we were particularly interested in unnatural amino acids containing a keto moiety, such as Acp and Bzp, to introduce a chemically reactive handle into GPCRs. Keto groups are generally absent from natural proteins, carbohydrates, and lipids and can be derivatized both *in vitro* (13, 30, 31) and *in vivo* (32–34) with hydrazide- or hydroxylamine-bearing probes under physiological conditions. For site-specific incorporation of Acp and Bzp into GPCRs in mammalian cells, we use two orthogonal pairs consisting of the *Bst*-Yam suppressor tRNA and *E. coli* TyrRS variants AcpRS (Y37I/D165G/D182G/F183M/L186A) and BzpRS (Y37G/D182G/L186A), respectively, developed earlier in yeast (18).

To adapt unnatural amino acid mutagenesis to low abundance membrane proteins, amber codon suppression by the orthogonal suppressor tRNA/aaRS pairs must be optimized and a clear assessment of the amount of functional protein that contains the unnatural amino acid is necessary. A highly sensitive assay based on firefly luciferase (FLuc) reporter was used to optimize transfection procedures, evaluate functional yields of mutant proteins, and confirm independently the orthogonality and specificity of these pairs in mammalian cells. We successfully incorporated Acp and Bzp efficiently into two different GPCRs, CCR5 and rhodopsin, targeting multiple specific sites while preserving the function of the mutant receptors. The functionality of the receptors was demonstrated by calcium flux assays and cell surface expression of CCR5, or by direct spectroscopic evaluation of rhodopsin. Furthermore, mutant rhodopsins containing Acp could be derivatized with a keto-reactive hydrazide-fluorophore. Our results highlight the general use of this approach to future biophysical and cell biological studies of 7-transmembrane receptors.

EXPERIMENTAL PROCEDURES

General—Standard *E. coli* genetic techniques were performed (35). *E. coli* strains XL1-Blue (*recA1 endA1 gyr96 thi-1 hsdR17 supE44 relA1 lac* (*F′ proAB* $lacI^qZ\Delta M15$ *Tn10 (Tet^r)*) from Stratagene and TOP10 (*F⁻ mcrA Δ(mrrr-hsdRMS-mcrBC) ϕ80lacZΔM15 ΔlacX74 recA1 araD139 Δ(ara-leu)7697 galU galK rpsL* (Str^R) *endA1 nupG*)) from Invitrogen were used for plasmid propagation and isolation. Oligonucleotides were obtained from IDT, Genelink, and eOligo. Plasmid DNA was purified using standard Maxi Prep or EndoFree Maxi Prep Kits from Qiagen. Acp and Bzp were from RSP Amino Acids LLC and Bachem, respectively.

Plasmids for Expression of Suppressor tRNA and Mutant aaRS Genes in Mammalian Cells—The expression cassette carrying an amber suppressor tRNA derived from the *B. stearothermophilus* $tRNA^{Tyr}$ (*Bst*-Yam) was designed with the following sequence: 5′-AGCGCTCCGGTTTTTCTGTGCTGAACCTCAGGGGACGCCGACACACGTACACGTCGGAGGGGTAGCGAAGTGGCTAAACGCGGCGGACTCTAAATCCGCTCCCTTTGGGTTCGGCGGTTCGAATCCGTCCCCCTCCA*GTCCTTTTTTTG*-3′. It consists of a (i) 5′ leader sequence taken from the human $tRNA^{Tyr}$ gene (underlined); (ii) the *B. stearothermophilus* $tRNA^{Tyr}$ gene sequence (bold) in which the anticodon was changed to

CUA (bold underlined) and the 3′-terminal CCA was omitted; and (iii) a 3′-terminal region containing a transcription termination sequence (italics). The expression cassette was amplified from a single-stranded DNA oligonucleotide by PCR and inserted into pSVBpUC (36). The gene encoding *E. coli* TyrRS was amplified by PCR from the genome of *E. coli* strain TOP10 and inserted into pBluescript II SK(+) (Stratagene) for subsequent mutagenesis. Mutations were introduced using the QuikChange multisite-directed mutagenesis kit (Stratagene) according to the manufacturer's protocol; Y37I/D165G/D182G/F183M/L186A for AcpRS and Y37G/D182G/L186A for BzpRS. The genes for AcpRS and BzpRS were further amplified by PCR introducing a C-terminal FLAG tag and cloned into the mammalian expression vector pCDNA3.1(+)/neo (Invitrogen).

Plasmids for Expression of FLuc, CCR5, and Rhodopsin in Mammalian Cells—The gene for wild-type firefly luciferase (FLuc.wt) and a variant thereof carrying a Y70am mutation (FLuc.Y70am) were amplified from plasmids described earlier (37) and inserted into the mammalian expression vector pCMVTNT (Promega). Both luciferase constructs contain a C-terminal His_6 tag. Plasmid pcDNA3.1(+)/neo carrying the gene for wild-type CCR5 (38) and plasmid pMT4 carrying the gene for wild-type rhodopsin were described earlier (39, 40). Both proteins contain a C-terminal 1D4 tag. Amber mutations were introduced into CCR5 at positions Ile-28, Phe-96, or Phe-260 using QuikChange mutagenesis (Stratagene). Similarly, rhodopsin mutants carrying an amber mutation at positions Tyr-29, Tyr-102, or Tyr-274 were generated. All plasmid constructs were confirmed by automated DNA sequencing.

Incorporation of Acp and Bzp into Proteins Expressed in Mammalian Cells—HEK293T and HEK293S *GnTI*$^-$ cells (41) were maintained in Dulbecco's modified Eagle's medium (4,500 mg/liter glucose, Invitrogen and Cellgro), 10% fetal bovine serum (Atlanta Biologicals), 2 mM glutamine, 100 units/ml penicillin, and 100 μg/ml streptomycin (Invitrogen) at 37 °C in a 5% CO_2 atmosphere. Mammalian cells were transfected with plasmid DNA using Lipofectamine Plus (Invitrogen) or Effectene (Qiagen). For transfection in a 10-cm culture dish, 3.5 μg of pcDNA.CCR5 (or pMT4.rho), 3.5 μg of pSVBpUC.*Bst*-Yam, and 0.35 μg of pcDNA.aaRS were mixed with Lipofectamine and added to cells at 70–80% confluence according to the manufacturer's protocol. Three hours after transfection, cells were fed with an equal volume of Dulbecco's modified Eagle's medium supplemented with 20% fetal bovine serum. Small scale transfections for luciferase expression in 24-well plates were carried out as described previously using Effectene (42). Unnatural amino acids were supplied at a final concentration of 0.3–1 mM 3 h post-transfection; Acp was dissolved directly in Dulbecco's modified Eagle's medium at a stock concentration of 2–3 mM; Bzp was neutralized with NaOH at a concentration of 0.2–0.4 M and then added to Dulbecco's modified Eagle's medium at a final concentration of 0.3–1 mM. Cells were harvested 48 h post-transfection and analyzed for expression of *Bst*-Yam, CCR5, rhodopsin, and luciferase.

Analysis of in Vivo State of Suppressor tRNAs Expressed in Mammalian Cells—Total RNAs were isolated under acidic conditions using TRIzol (Invitrogen). The tRNA was resuspended in 10 mM sodium acetate, pH 5.0, and stored in 10 mM sodium acetate, pH 5.0, at −80 °C. tRNAs were separated by acid urea PAGE (43), electroblotted onto Nytran-SPC membrane (Whatman), and detected by standard Northern blot hybridization. Membranes were prehybridized at 42 °C in 10× Denhardt's solution/6× SSC/0.5% SDS. Hybridization was performed at 42 °C in 6× SSC/0.1% SDS in the presence of a 5′-^{32}P-labeled oligonucleotide complementary to nucleotides 1–20 of the *Bst*-Yam suppressor tRNA. An oligonucleotide complementary to nucleotides 18–36 of the human initiator $tRNA_i^{Met}$ was used as an internal standard. Membranes were washed at room temperature, once with 6× SSC/0.1% SDS followed by two washes with 6× SSC, and then subjected to autoradiography. Northern blots were quantified by PhosphorImager analysis using ImageQuaNT software (Molecular Dynamics).

Assay for Luciferase Activity—A Single Luciferase Reporter System (Promega) was used to assay luciferase activity following the manufacturer's instructions. The preparation of mammalian cell extracts has been described elsewhere (37). Measurement of luciferase activities was carried out on a Sirius tube luminometer (Berthold Detection Systems) with a 10-s premeasurement delay and a 15-s measurement period. Luciferase activities are given as relative luminescence units per μg of total cell protein. The protein concentration of cell lysates was determined with a BCA protein assay (Pierce) using BSA as standard. The values shown in the tables and figures represent the averages of at least two independent experiments; variation among experiments was <10%.

Immunoblot Analysis—Cell lysates were resolved by SDS-PAGE and transferred onto Immobilon, a polyvinylidene difluoride membrane (Millipore), according to the protocols provided by the manufacturer. The membranes were probed with primary antibodies against the 1D4 epitope (National Cell Culture Center, 1:5,000), His_4 tag (Qiagen; 1:5,000), FLAG tag (Invitrogen; 1:5,000), and a horseradish peroxidase-conjugated secondary antibody (Amersham Biosciences GE or KPL Inc.; 1:5,000 to 1:10,000; anti-mouse IgG). Signals were visualized by enhanced chemiluminescence treatment (Amersham Biosciences GE or PerkinElmer Life Sciences) and exposure to X-Omat AR film (Eastman Kodak). Equal amounts of total protein were analyzed per lane.

Characterization of RANTES-dependent Calcium Flux in Transiently Transfected HEK293T Cells—Assays of calcium flux in mammalian cells using Fluo-3 (Invitrogen) as an intracellular calcium-indicator dye were performed essentially as described (44). Studies were performed at least twice on independent samples. Dose-response data were collected by measuring the effects of various concentrations of human RANTES peptide (Peprotech) on the calcium flux. For each concentration, 10% (v/v) Triton X-100 was added to lyse the cells for maximal fluorescence followed by a quench with 4 mM EGTA that provides the minimal signal. Fluorescence was measured on an F-4500 Fluorescence Spectrophotometer (Hitachi). Fluorescence peak heights normalized to the total fluorescence response were plotted against RANTES concentration, and the data were fit to a four-parameter logistic function of the form: $f(x) = a + [(b - a)/(1 + (x/c)^d)]$ (45). The EC_{50} values were calculated from the inflection point c of the best-fit curve.

Cell Surface Expression of CCR5 and Fluorescence Microscopy—24 h post-transfection, cells were plated on 12-mm glass coverslips coated with poly-L-lysine and cultured for another 24 h. Cells were fixed with 4% paraformaldehyde and labeled either with fluorescein isothiocyanate-conjugated anti-CCR5 antibody (clone 2D7, BD Pharmingen) or with 1D4 antibody followed by Alexa 488-conjugated anti-mouse IgG secondary antibody. Fluorescence images of permeabilized and non-permeabilized cells were obtained. The cells were imaged on a Zeiss Axiovert 200M inverted microscope using a 20× objective. The images were acquired using Axiovision software and processed using Adobe Photoshop.

Preparation and Spectral Characterization of Rhodopsin Mutants—The regeneration, immunoaffinity purification, and UV-visible absorption spectroscopy of rhodopsin were performed as described (39, 46). Rhodopsin samples were generally obtained in 0.1% (w/v) *n*-dodecyl-β-D-maltoside (DM, Anatrace)/0.1 M sodium phosphate (pH 6.5). UV-visible spectra were recorded with a Lambda 800 spectrophotometer (PerkinElmer Life Sciences) set to a slit width of 2 nm in a cuvette with a 1-cm path length before and after 30 s of photobleaching with a 150-W FiberLite A-200 fiber-optic light source (Dolan Jenner Industries) using a 495-nm cut-off filter. The intensity of the 500 nm peak was used to calculate the concentration of rhodopsin, with an extinction coefficient of 42,000 $M^{-1}cm^{-1}$.

Site-specific Labeling in Vitro of Purified Rhodopsin Mutants Containing a Reactive Keto Moiety—Cells from a 10-cm culture dish were harvested, regenerated with 11-*cis*-retinal, and further solubilized with 1 ml of SB buffer (0.05 M HEPES, 0.1 M NaCl, 1 mM $CaCl_2$, pH 6.8) containing 1.0% (w/v) DM for 3–4 h at 4 °C as described (39). After centrifugation at 30,000 × *g* for 30 min, supernatant fractions were loaded onto 50 μl of 1D4 resin slurry (39) and equilibrated for ~4 h at 4 °C. Resins were washed three times with WB1 (0.05 M HEPES, 0.1 M NaCl, 0.05% DM, pH 6.0), and then incubated with 300 μl of WB1 containing 1 mM fluorescein-hydrazide (Invitrogen) overnight at room temperature. Resins were washed extensively with WB1 (pH 6.8), followed by washes with WB2 (0.1 M sodium phosphate, 0.1% DM, pH 6.5). Labeled rhodopsin was eluted in a total volume of ~100 μl of EB (WB2 buffer containing 0.36 mg/ml 1D5 peptide, Anaspec). Samples were analyzed by UV-visible spectroscopy and subsequently subjected to SDS-PAGE. The amount of rhodopsin was normalized based on the absorbance at 500 nm. Gels were imaged using a Typhoon 9400 Image Scanner (Amersham Biosciences GE) with an excitation (488 nm)/emission (520 nm BP40) filter-set optimized for fluorescein detection.

RESULTS

Evaluation of Mutant TyrRS/Bst-Yam Pairs in Mammalian Cells—HEK293T cells were co-transfected with plasmids carrying the respective genes for *Bst*-Yam, *E. coli* TyrRS (wild-type, AcpRS, or BzpRS), and the FLuc reporter containing an amber codon at position Y70 (FLuc.Y70am) (Table 1). FLuc activity measured in total cell extracts strictly depended on the co-expression of both *Bst*-Yam and TyrRS confirming the orthogonality of the suppressor tRNA in mammalian cells (Table 1, rows 1–4). In the presence of wild-type TyrRS, suppression efficiencies were in the range of ~35% corresponding to ~0.5 μg of FLuc/10^5 cells (data not shown). Co-expression of *Bst*-Yam and TyrRS mutants AcpRS or BzpRS in the presence of 0.3 mM Acp or Bzp led to efficient incorporation of the respective analogue into the luciferase reporter, with suppression efficiencies of ~18% for AcpRS (Table 1, row 7) and ~8% for BzpRS (Table 1, row 11). Some minor readthrough in the absence of Acp suggests some misincorporation of tyrosine by AcpRS (Table 1, row 5), whereas BzpRS was much more specific for Bzp (Table 1, row 9). The data based on FLuc activity were corroborated by immunoblot analysis (supplemental Fig. S1). The amount of full-length FLuc protein corresponded to the levels of luciferase activity measured in the same samples. Furthermore, immunoblotting confirmed that wild-type and mutant TyrRSs were expressed to similar levels (supplemental Fig. S1).

TABLE 1

Site-specific insertion of Acp or Bzp into firefly luciferase in mammalian cells

HEK293T cells were transfected with plasmids carrying the genes for FLuc (wild-type or FLuc.Y70am), *Bst*-Yam, and *E. coli* TyrRS (wild-type, AcpRS, or BzpRS), and cultured in the absence and presence of Acp or Bzp at a final concentration of 0.3 mM. Cells were harvested 48 hours post-transfection and analyzed for FLuc activity as described (37). The average FLuc activities from two independent experiments are described as relative luminescence units (RLU)/μg of protein in a total cell extract and as percentage of wild-type activity (%).

	FLuc	tRNA	TyrRS	aa[a]	FLuc activity	Relative FLuc activity
					× 10^6 (RLU/μg)	%
1	Y70am				0.03	0.01
2	Y70am	Yam			0.88	0.35
3	Y70am	Yam	wt		86.60	34.53
4	wt	Yam	wt		250.82	100.00
5	Y70am	Yam	AcpRS		4.14	1.34
6	wt	Yam	AcpRS		308.92	100.00
7	Y70am	Yam	AcpRS	Acp	53.40	17.34
8	wt	Yam	AcpRS	Acp	307.88	100.00
9	Y70am	Yam	BzpRS		0.89	0.24
10	wt	Yam	BzpRS		361.53	100.00
11	Y70am	Yam	BzpRS	Bzp	15.34	7.75
12	wt	Yam	BzpRS	Bzp	198.75	100.00

[a] aa, amino acid.

We also examined the expression of the *Bst*-Yam suppressor tRNA and the extent of its aminoacylation *in vivo*. Total RNA was isolated from HEK293T cells under acidic conditions and subjected to analysis by acid urea PAGE followed by Northern blotting (43) using a ^{32}P-labeled DNA oligonucleotide complementary to *Bst*-Yam (Fig. 1). Cells transfected with plasmid pSVBpUC carrying the *Bst*-Yam gene show a clear signal corresponding to the expression of mature suppressor tRNA (Fig. 1, *lane 2*). As expected, *Bst*-Yam was not aminoacylated in the absence of *E. coli* TyrRS, its aminoacylation depended strictly upon co-expression of wild-type TyrRS (~75%), AcpRS (~65%), or BzpRS (~50%) and the corresponding unnatural amino acid (Fig. 1, *lanes 3*, *5*, and *7*). AcpRS aminoacylates the *Bst*-Yam suppressor tRNA *in vivo* at a low level in the absence of Acp (Fig. 1, *lane 4*), consistent with the data above indicating some minor background FLuc activity in the absence of Acp (Table 1, *lane 5*). All samples show a small amount of non- or partially processed *Bst*-Yam precursor as a slower migrating band.

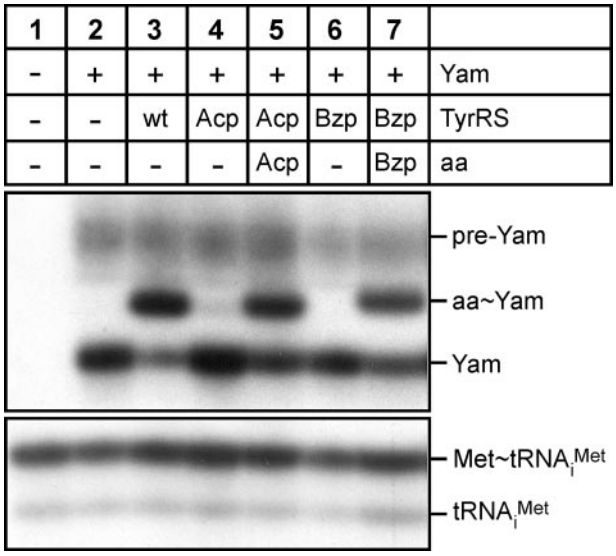

FIGURE 1. ***In vivo* aminoacylation state of *Bst*-Yam suppressor tRNA in mammalian cells.** Total RNA was isolated under acidic conditions from HEK293T cells transfected with plasmids carrying the genes for *Bst*-Yam and *E. coli* TyrRS (wild-type, AcpRS, or BzpRS). Cells were cultured in the absence and presence of Acp or Bzp as indicated. tRNAs were analyzed by acid urea PAGE followed by Northern hybridization using a DNA oligonucleotide specific for *Bst*-Yam. An oligonucleotide specific for the human initiator tRNA$_i^{Met}$ was used as internal standard for quantitation of RNA and aminoacylation levels by PhosphorImager analysis. *aa*, amino acid; *pre-Yam*, *Bst*-Yam precursor.

Site-specific Incorporation of Acp into CCR5—We first attempted the incorporation of Acp into CCR5 at position F260 (CCR5-F260Acp), located in the extracellular loop E3 (Fig. 2*A*). The expression of CCR5-F260Acp in HEK293T cells was analyzed in detail by immunoblotting and functional readout by calcium flux using wild-type CCR5 as a control (Fig. 2, *B–D*). CCR5-F260Acp was synthesized only in those cells co-expressing *Bst*-Yam and AcpRS in the presence of exogenously added Acp (Fig. 2*B*, *lane 5*). In the absence of any of these components, we observed no full-length CCR5 by immunoblot analysis and only negligible RANTES-dependent calcium flux (Fig. 2*C*, *lanes 2–4*). The measurement of calcium flux allowed us to quantitate the level of functional CCR5-F260Acp, which was consistently found to be greater than 30% compared with wild-type CCR5 (Fig. 2*C*, *lanes 1* and *5*). Dose-response studies on CCR5-F260Acp with a titration of RANTES from 0 to −400 nM demonstrated that the incorporation of Acp did not affect RANTES binding (Fig. 2*D*). The EC_{50} value was calculated to be 7.3 nM, based on the average from three independent transfection experiments, and compares well with the experimental value for wild-type CCR5 of 2.2 nM (see Fig. 3, *lane 1*) and the reported value of 3.0 nM (47). Immunofluorescence studies using antibodies specific for the N- and C-terminal domains of CCR5 confirmed that the mutant receptor containing Acp was properly displayed at the cell surface (Fig. 2*E*).

Expression of Functionally Active CCR5 Mutants Containing Acp or Bzp at Three Different Positions—We next studied the incorporation of Acp and Bzp into CCR5 at three different target sites in the N terminus and extracellular loops E1 and E3, respectively (Ile-28, Phe-96, and Phe-260, Figs. 2*A* and 3). Immunoblot analysis showed that, in general agreement with the incorporation of Acp and Bzp into FLuc (Table 1), CCR5 mutants containing Acp were produced to ~50% compared with wild-type and to significantly higher levels (> 5-fold) than those containing Bzp (Fig. 3, compare *lanes 3–5* with *lanes 6–8*). Interestingly, the functional readouts based on calcium flux did not follow the same trend. For example, CCR5 mutants F96Bzp and F260Bzp show a calcium flux greater than 50% compared with wild-type CCR5, whereas the amount of protein detected is significantly less (Fig. 3, *lanes 1*, *7*, and *8*). Likewise, CCR5-I28Acp and CCR5-I28Bzp produce a similar calcium flux of ~ 30%, yet CCR5-I28Bzp is barely detectable by immunoblotting in contrast to CCR5-I28Acp (Fig. 3, *lanes 3* and *6*). Average yields of CCR5 synthesis were calculated (supplemental Table S2). EC_{50} values were determined for all CCR5 mutants, these ranged from 1.3 to 7.3 nM (Fig. 3, *bottom line*) suggesting that the incorporation of Acp or Bzp into CCR5 at Ile-28, Phe-96, or Phe-260 positions did not perturb the overall RANTES-dependent signaling activity of the mutant receptors. Also, all six mutant receptors were localized to the cell surface (supplemental Fig. S2). The disparity in the yields measured by immunoblot *versus* RANTES-dependent calcium flux suggests that the expression level of full-length receptors does not necessarily correlate with the level of functional receptors measured by downstream second-messenger readouts. A complete characterization of this interesting phenomenon is in progress. Overall, our results are very promising in that we observe efficient amber suppression at various target sites and consequently efficient synthesis of receptor proteins containing Acp or Bzp.

Site-specific Incorporation of Keto Amino Acids into Rhodopsin and in Vitro Labeling of Rhodopsin Mutants—To evaluate the generality of producing high yields of GPCRs that contain Acp or Bzp, we also tested rhodopsin, one of the few GPCRs that can be purified easily, while preserving its full functionality. We incorporated Acp into the extracellular loop E1 at position Tyr-102 (Fig. 2*A*), a site known to be solvent-accessible based on the crystal structure and dynamics simulations (5, 48, 49). Rhodopsin containing Acp (rho-Y102Acp) was purified from transiently transfected HEK293S *GnTI*$^-$ cells (41) and analyzed by UV-visible absorbance spectroscopy before and after photobleaching (Fig. 4*A*). The difference spectra of wild-type rhodopsin and rho-Y102Acp were used to assess the functionality of the receptors (Fig. 4*A*, *inset*). As expected, no detectable spectral shift was observed for rho-Y102Acp confirming that the incorporation of Acp did not affect the native chromophore binding pocket. The relative absorbance at 500 nm showed that the rho-Y102Acp mutant was produced at a remarkable 42% compared with wild-type rhodopsin. The average yield of rho-Y102Acp isolated from a single 10-cm plate (~10^7 cells) was ~2 μg.

To demonstrate covalent *in vitro* labeling of the keto moiety with fluorescein-hydrazide under mild acidic conditions, we synthesized three different rhodopsin mutants containing Acp (rho-Y29Acp, rho-Y102Acp, and rho-Y274Acp (Fig. 2*A* and supplemental Table S2)). Fluorescein-labeled rhodopsin samples were separated by SDS-PAGE and visualized under a fluorescence image scanner (Fig. 4*B*). A strong fluorescent signal was observed for all three mutant receptors, significantly stronger than the background signal seen for wild-

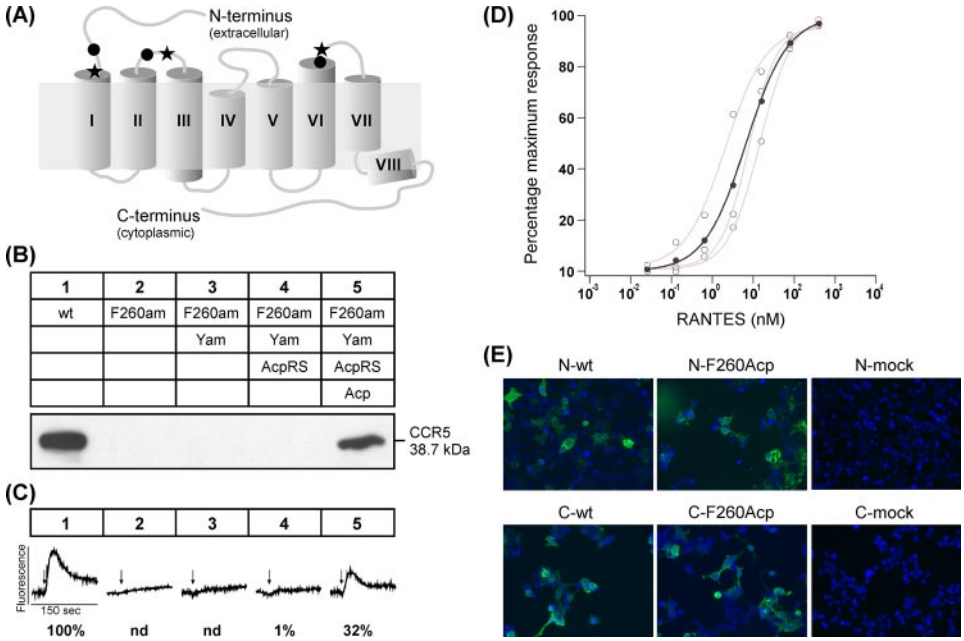

FIGURE 2. **Site-specific incorporation of Acp into functional CCR5 in mammalian cells.** *A*, schematic representation of the secondary structure of CCR5 and rhodopsin. The 7-transmembrane helices (*I–VII*) and the cationic amphipathic helix VIII are shown as *cylinders*. Positions in CCR5 (★) and rhodopsin (●) subjected to site-specific incorporation of unnatural amino acids are indicated. *B*, analysis of cell lysates by immunoblot using an antibody against the C-terminal 1D4 epitope of CCR5. HEK293T cells were transfected with plasmids encoding CCR5-wt or CCR5-F260am, *Bst*-Yam, and AcpRS. Cells were cultured in the absence and presence of Acp as indicated. Equal amounts of total protein were analyzed per *lane*. *C*, ligand-induced calcium flux. *Traces* represent the levels of Fluo-3 fluorescence emitted over time by cells in suspension (44). The addition of RANTES (20 nM) is indicated by *arrows*. Relative CCR5 activities are summarized underneath. *D*, dose-response curves of CCR5-F260Acp. Calcium flux was measured at various concentrations of RANTES ranging from 0 to 400 nM; the data from three independent measurements (*gray*) were normalized and averaged (*black*) as described (45). *E*, cell surface expression of CCR5-wt and CCR5-F260Acp. Fluorescence images of non-permeabilized cells labeled with a fluorescein isothiocyanate-conjugated anti-CCR5 antibody against the extracellular N-terminal 2D7 epitope of CCR5 (*N*, *top panel*), and permeabilized cells were labeled with an antibody against the cytoplasmic C-terminal 1D4 tag (*C*, *bottom panel*) of CCR5 followed by staining with an Alexa 488-conjugated secondary antibody. *Blue*, nuclei stained with 4′,6-diamidino-2-phenylindole; *green*, labeled CCR5.

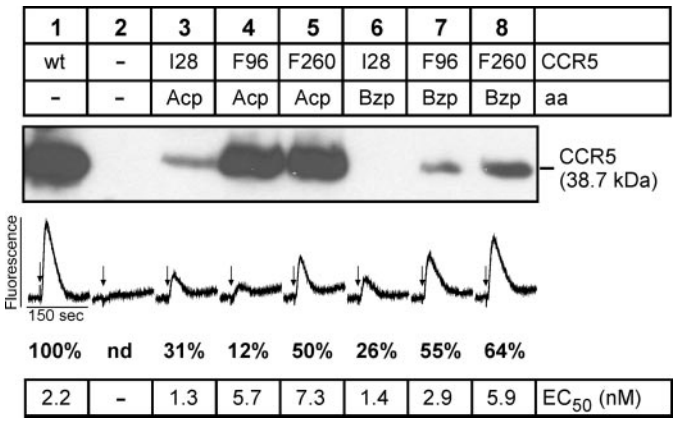

FIGURE 3. **Expression of functional CCR5 mutants containing Acp or Bzp at positions 28, 96, or 260.** HEK293T cells were transfected with plasmids carrying the genes for CCR5-wt or CCR5 mutant with an amber mutation at position Ile-28, Phe-96, or Phe-260. Plasmids encoding *Bst*-Yam and *E. coli* TyrRS (AcpRS or BzpRS) were co-transfected, and the corresponding unnatural amino acids (Acp or Bzp) were provided in the cell media as indicated. Cell lysates were analyzed by immunoblot using an antibody against the C-terminal 1D4 epitope of CCR5 (*top*) and RANTES-induced calcium flux (*bottom*). Equal amounts of total protein were analyzed per lane. Calcium flux traces represent the levels of Fluo-3 fluorescence emitted over time by cells in suspension (44). The addition of RANTES (20 nM) is indicated by *arrows*. Relative CCR5 activities and EC_{50} values for RANTES-induced calcium flux are summarized underneath.

type rhodopsin treated under the same conditions. Fluorescein-labeled rhodopsins were also analyzed by UV-visible spectroscopy confirming normal chromophore regeneration and bleaching behavior of the labeled receptors (Fig. 4*C* and supplemental Fig. S3). Labeling efficiencies are provided as molar ratios of fluorescein to rhodopsin mutant (Fig. 4*D*).

DISCUSSION

We introduced keto-containing unnatural amino acids Acp and Bzp at specific sites in 7-transmembrane receptors CCR5 and rhodopsin in mammalian cells using amber suppression by orthogonal *E. coli* mutant aaRS/*Bst*-Yam suppressor tRNA pairs. The remarkably high yield of 0.5–2 μg of Acp-containing rhodopsins/10^7 cells can be attributed to the efficient synthesis of both the mutant aaRS and the suppressor tRNA optimized by the convenient screening of various tRNA and aaRS gene constructs and transfection procedures using the luciferase assay (data not shown). The extent of *in vivo* aminoacylation of the *Bst*-Yam suppressor tRNA was found to vary from ~65% with Acp to ~50% with Bzp, compared with ~75% with tyrosine. Given the approximately similar level of aminoacylated *Bst*-Yam *in vivo*, the difference in yields of FLuc and CCR5 containing Acp, Bzp, or tyrosine (Table 1 and Fig. 2) could reflect the discrimination by components of the translational machinery such as the elongation factor and/or ribosome toward these unnatural amino acids.

We focused our attention on unnatural amino acid mutagenesis in mammalian cells because, despite intense efforts for decades, expression of functional GPCRs in *E. coli* has not been possible. We introduced non-perturbing but reactive keto-containing amino acids, Acp and Bzp, for subsequent derivatization. Bzp also has the added advantage of being a potent photochemical cross-linking agent, which would facilitate identification of sites of protein-protein interactions and intra- and intermolecular conformational dynamics studies. For example, photo-cross-linking could be used to identify the precise sites of GPCR docking to G proteins and arrestins and for understanding the molecular basis of ligand recognition by chemokine receptors. The presence of keto-reactive groups at specific sites in proteins provides virtually unlimited potential to attach labels with specific properties best suited for a variety of spectroscopic methods, including Fourier transform IR, EPR, and NMR. The only limiting factor is the amount of functional labeled receptor that can be obtained.

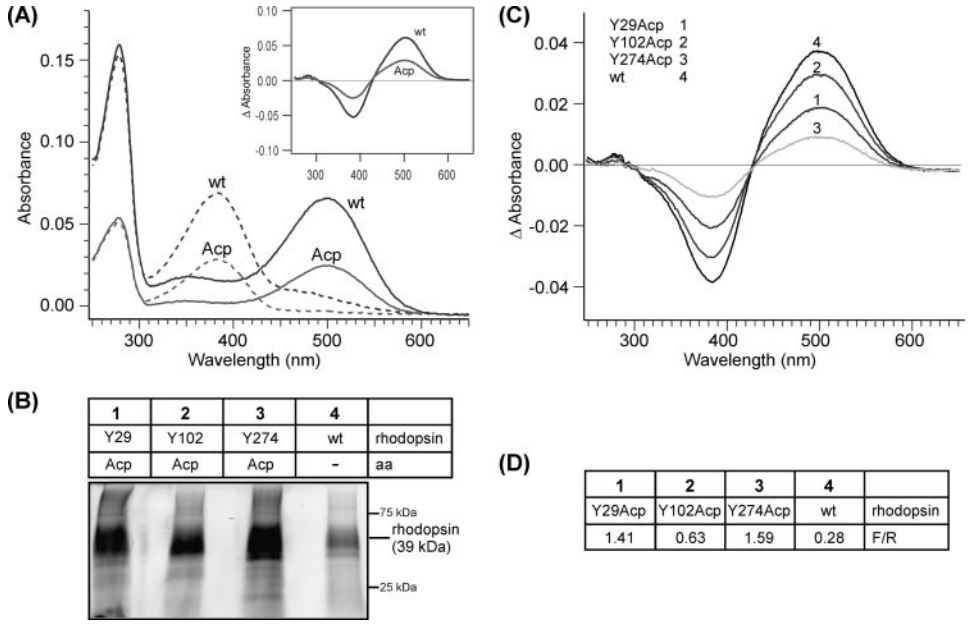

FIGURE 4. **Site-specific incorporation of Acp into rhodopsin and *in vitro* labeling of rhodopsin mutants.** *A*, UV-visible spectra for purified wild-type (*black*) and mutant rhodopsin containing Acp (*gray*) at position 102 were taken in the dark (*solid lines*) and after photobleaching (*dashed lines*) as described (39, 46). Difference spectra (*inset*) were generated by subtracting the photobleached spectra from the dark spectra. *B*, *in vitro* labeling of rhodopsin mutants (rho-Y29Acp, rho-Y102Acp, and rho-Y274Acp) with fluorescein-hydrazide. Rhodopsin concentrations were confirmed by difference UV-visible spectra, and the loading volume was normalized to the same amount of rhodopsin based on the 500 nm absorbance (supplemental Fig. S3). Samples were separated by 12% SDS-PAGE; the fluorescence image was taken with a Typhoon 9400 Image Scanner using an excitation/emission filter set optimized for fluorescein detection. *C*, photobleaching difference spectra of rhodopsins treated with fluorescein hydrazide. *1*, rho-Y29Acp; *2*, rho-Y102Acp; *3*, rho-Y274Acp; and *4*, wild-type. *D*, stoichiometric ratios of fluorescein/rhodopsin were determined after normalizing the amount of rhodopsin based on the absorbance at 500 nm. The molar extinction coefficients used for calculations were 42,000 $M^{-1}cm^{-1}$ for rhodopsin and 93,200 $M^{-1}cm^{-1}$ for fluorescein. *F/R*, fluorescein/rhodopsin molar ratio.

With rhodopsin, we have shown direct *in vitro* chemical labeling of the Acp-containing mutant rhodopsins by fluorescein-hydrazide (Fig. 4), which is specific to the keto moiety. Furthermore, with isolation of 0.5–2 μg of Acp-containing rhodopsin from $\sim 10^7$ cells, tens of micrograms of specifically labeled rhodopsins can be prepared routinely, allowing for a wide variety of biochemical, biophysical, and spectroscopic studies. The yields of mutant rhodopsins are remarkable for a membrane protein carrying an unnatural amino acid given the fact that the only reported yield for a soluble protein (green fluorescent protein) is in the range of 0.5 $\mu g/10^7$ cells (19). Additionally, with the generation of appropriate stable cell lines and use of a bioreactor, it should be possible to generate tens of milligrams of mutant rhodopsins carrying unnatural amino acids at specific sites (50).

Chemokine receptors are an exceedingly important sub-class of GPCRs; certain receptors are involved in cell migration during development, mediate inflammation, and act as human immunodeficiency virus, type 1 co-receptors (38). We prepared six distinct CCR5 mutants, with either Acp or Bzp at one of three positions on the extracellular surface region, and showed that each of the six CCR5 mutants trafficked to the cell surface. Our aim was to introduce unnatural amino acids at functionally neutral sites. However, it is interesting that CCR5-I28Acp and I28Bzp displayed EC_{50} values for ligand (RANTES)-dependent calcium flux that were somewhat lower than wild-type CCR5. This raises the possibility that the presence of Acp or Bzp at position 28 enhances the affinity for RANTES. In some cases, we observed a robust calcium flux signal despite sparing amounts of mutant CCR5 detected by immunoblot analysis. This discrepancy is not totally unexpected given the fact that immunoblot analysis detects the total amount of receptors, regardless of the functional state, while the calcium flux assay measures only the presence of functional receptors at the plasma membrane surface. However, it is also possible that Bzp enhances the interaction of RANTES with CCR5 directly. The overall suppression yield for various CCR5 constructs was exceptional, up to 60% compared with wild-type using RANTES-induced calcium flux as a functional readout (Fig. 3). At these expression levels, it should be possible to carry out direct live cell surface labeling of the keto moiety on the extracellular surface of a CCR5 mutant. We are currently pursuing both *in vitro* and *in vivo* fluorescent labeling approaches. Also, site-specific incorporation of *p*-azido-L-phenylalanine is planned to test an alternative labeling chemistry involving Staudinger-Bertozzi ligation (51).

Crystal structures of β2-adrenergic receptor were recently reported (52–54). In much the same way as the elucidation of the three-dimensional structure of ribosomes (55–58), triggered a rejuvenation of biochemical and functional studies on ribosomes and protein synthesis in general, the availability of these adrenergic receptor structures will provide a major impetus for additional work on GPCRs and aspects of signal transduction. Although these new structures, together with earlier crystal structures of rhodopsin, represent an important advance in understanding the large Type I (rhodopsin-like) GPCR family, they capture only static snapshots of inverse agonist-bound ground states. Additional biophysical and functional studies will be necessary, for example, to understand how ligand molecules are recognized specifically (affinity) and how ligand binding events alter receptor conformational dynamics to form an active state (efficacy), which can complex with a heterotrimeric G protein.

We were particularly interested in developing a framework for single-molecule fluorescence studies, which requires the availability of homogeneously labeled proteins with labels at one or more sites. Although site-specific cysteine/maleimide labeling has been used extensively, the method is not entirely general. However, we anticipate that a combination of cysteine labeling and unnatural amino acid

mutagenesis will provide the basis for discrete double labeling of individual receptors with two different fluorophores, which would facilitate fluorescence resonance energy transfer-based studies. We are currently studying the mechanism of chemokine ligand binding to CCR5 reconstituted in tethered and oriented membrane systems by single-molecule fluorescence. We aim to employ CCR5 with fluorescent labels introduced at specific reactive unnatural amino acid residues to demonstrate ligand-dependent conformational changes in the receptor, and in combination with labeled chemokines, to determine the orientation of the ligand-receptor complex by fluorescence resonance energy transfer. The work described in this report highlighting the potential application of unnatural amino acid mutagenesis to GPCRs makes such studies possible.

In conclusion, we have optimized and characterized a robust system for unnatural amino acid mutagenesis and have used it to introduce Acp and Bzp, two keto-containing amino acids, at multiple sites in two different GPCRs. We demonstrate the efficiency of the system by direct functional comparison with wild-type receptors expressed under the same conditions. We foresee that combining the unnatural amino acid mutagenesis with novel labeling chemistries will provide a powerful tool to study the molecular architecture and ligand-induced conformational changes in GPCRs and to elucidate their complex cellular trafficking dynamics.

Acknowledgments—We thank Christoph Seibert, Sourabh Banerjee, and Jay Janz for invaluable discussions. We are also grateful to the Proteomic Resource Center at The Rockefeller University for providing technical resources and support.

REFERENCES

1. Pierce, K. L., Premont, R. T., and Lefkowitz, R. J. (2002) *Nat. Rev. Mol. Cell. Biol.* **3,** 639–650
2. Lefkowitz, R. J. (2004) *Trends Pharmacol. Sci.* **25,** 413–422
3. Lefkowitz, R. J. (2007) *Biochim. Biophys. Acta* **1768,** 748–755
4. Sakmar, T. P., Menon, S. T., Marin, E. P., and Awad, E. S. (2002) *Annu. Rev. Biophys. Biomol. Struct.* **31,** 443–484
5. Palczewski, K., Kumasaka, T., Hori, T., Behnke, C. A., Motoshima, H., Fox, B. A., Le Trong, I., Teller, D. C., Okada, T., Stenkamp, R. E., Yamamoto, M., and Miyano, M. (2000) *Science* **289,** 739–745
6. Farrens, D. L., Altenbach, C., Yang, K., Hubbell, W. L., and Khorana, H. G. (1996) *Science* **274,** 768–770
7. Imamoto, Y., Kataoka, M., Tokunaga, F., and Palczewski, K. (2000) *Biochemistry* **39,** 15225–15233
8. Gether, U., Lin, S., Ghanouni, P., Ballesteros, J. A., Weinstein, H., and Kobilka, B. K. (1997) *EMBO J.* **16,** 6737–6747
9. Payne, R. C., Nichols, B. P., and Hecht, S. M. (1987) *Biochemistry* **26,** 3197–3205
10. Bain, J. D., Glabe, C. G., Dix, T. A., and Chamberlin, A. R. (1989) *J. Am. Chem. Soc.* **111,** 8013–8014
11. Noren, C. J., Anthony-Cahill, S. J., Griffith, M. C., and Schultz, P. G. (1989) *Science* **244,** 182–188
12. Cornish, V. W., Benson, D. R., Altenbach, C. A., Hideg, K., Hubbell, W. L., and Schultz, P. G. (1994) *Proc. Natl. Acad. Sci. U. S. A.* **91,** 2910–2914
13. Cornish, V. W., Hahn, K. M., and Schultz, P. G. (1996) *J. Am. Chem. Soc.* **118,** 8150–8151
14. Wang, L., Brock, A., Herberich, B., and Schultz, P. G. (2001) *Science* **292,** 498–500
15. Kiga, D., Sakamoto, K., Kodama, K., Kigawa, T., Matsuda, T., Yabuki, T., Shirouzu, M., Harada, Y., Nakayama, H., Takio, K., Hasegawa, Y., Endo, Y., Hirao, I., and Yokoyama, S. (2002) *Proc. Natl. Acad. Sci. U. S. A.* **99,** 9715–9720
16. Sakamoto, K., Hayashi, A., Sakamoto, A., Kiga, D., Nakayama, H., Soma, A., Kobayashi, T., Kitabatake, M., Takio, K., Saito, K., Shirouzu, M., Hirao, I., and Yokoyama, S. (2002) *Nucleic Acids Res.* **30,** 4692–4699
17. Beene, D. L., Dougherty, D. A., and Lester, H. A. (2003) *Curr. Opin. Neurobiol.* **13,** 264–270
18. Chin, J. W., Cropp, T. A., Anderson, J. C., Mukherji, M., Zhang, Z., and Schultz, P. G. (2003) *Science* **301,** 964–967
19. Liu, W., Brock, A., Chen, S., Chen, S., and Schultz, P. G. (2007) *Nat. Methods* **4,** 239–244
20. Wang, W., Takimoto, J. K., Louie, G. V., Baiga, T. J., Noel, J. P., Lee, K. F., Slesinger, P. A., and Wang, L. (2007) *Nat. Neurosci.* **10,** 1063–1072
21. Hino, N., Okazaki, Y., Kobayashi, T., Hayashi, A., Sakamoto, K., and Yokoyama, S. (2005) *Nat. Methods* **2,** 201–206
22. Zhang, Z., Alfonta, L., Tian, F., Bursulaya, B., Uryu, S., King, D. S., and Schultz, P. G. (2004) *Proc. Natl. Acad. Sci. U. S. A.* **101,** 8882–8887
23. Heckler, T. G., Chang, L. H., Zama, Y., Naka, T., Chorghade, M. S., and Hecht, S. M. (1984) *Biochemistry* **23,** 1468–1473
24. Nowak, M. W., Kearney, P. C., Sampson, J. R., Saks, M. E., Labarca, C. G., Silverman, S. K., Zhong, W., Thorson, J., Abelson, J. N., Davidson, N., *et al.* (1995) *Science* **268,** 439–442
25. Lummis, S. C., Beene, D. L., Harrison, N. J., Lester, H. A., and Dougherty, D. A. (2005) *Chem. Biol.* **12,** 993–997
26. Turcatti, G., Nemeth, K., Edgerton, M. D., Meseth, U., Talabot, F., Peitsch, M., Knowles, J., Vogel, H., and Chollet, A. (1996) *J. Biol. Chem.* **271,** 19991–19998
27. Edwards, H., and Schimmel, P. (1990) *Mol. Cell. Biol.* **10,** 1633–1641
28. Drabkin, H. J., Park, H. J., and RajBhandary, U. L. (1996) *Mol. Cell. Biol.* **16,** 907–913
29. Kowal, A. K., Köhrer, C., and RajBhandary, U. L. (2001) *Proc. Natl. Acad. Sci. U. S. A.* **98,** 2268–2273
30. Bayer, E. A., Ben-Hur, H., and Wilchek, M. (1988) *Anal. Biochem.* **170,** 271–281
31. Wang, L., Zhang, Z., Brock, A., and Schultz, P. G. (2003) *Proc. Natl. Acad. Sci. U. S. A.* **100,** 56–61
32. Mahal, L. K., Yarema, K. J., and Bertozzi, C. R. (1997) *Science* **276,** 1125–1128
33. Chen, I., Howarth, M., Lin, W., and Ting, A. Y. (2005) *Nat. Methods* **2,** 99–104
34. Zhang, Z., Smith, B. A., Wang, L., Brock, A., Cho, C., and Schultz, P. G. (2003) *Biochemistry* **42,** 6735–6746
35. Sambrook, J., Fritsch, E. F., and Maniatis, T. (1989) *Molecular Cloning: A Laboratory Manual*, 2nd Ed., Cold Spring Harbor Laboratory Press, Cold Spring Harbor, NY
36. Drabkin, H. J., and RajBhandary, U. L. (1985) *J. Biol. Chem.* **260,** 5588–5595
37. Köhrer, C., Yoo, J., Bennett, M., Schaack, J., and RajBhandary, U. L. (2003) *Chem. Biol.* **10,** 1095–1102
38. Seibert, C., Ying, W., Gavrilov, S., Tsamis, F., Kuhmann, S. E., Palani, A., Tagat, J. R., Clader, J. W., McCombie, S. W., Baroudy, B. M., Smith, S. O., Dragic, T., Moore, J. P., and Sakmar, T. P. (2006) *Virology* **349,** 41–54
39. Min, K. C., Zvyaga, T. A., Cypess, A. M., and Sakmar, T. P. (1993) *J. Biol. Chem.* **268,** 9400–9404
40. Karnik, S. S., Sakmar, T. P., Chen, H. B., and Khorana, H. G. (1988) *Proc. Natl. Acad. Sci. U. S. A.* **85,** 8459–8463
41. Reeves, P. J., Callewaert, N., Contreras, R., and Khorana, H. G. (2002) *Proc. Natl. Acad. Sci. U. S. A.* **99,** 13419–13424
42. Köhrer, C., Sullivan, E. L., and RajBhandary, U. L. (2004) *Nucleic Acids Res.* **32,** 6200–6211
43. Varshney, U., Lee, C. P., and RajBhandary, U. L. (1991) *J. Biol. Chem.* **266,** 24712–24718
44. Cypess, A. M., Unson, C. G., Wu, C. R., and Sakmar, T. P. (1999) *J. Biol. Chem.* **274,** 19455–19464
45. Kazmi, M. A., Snyder, L. A., Cypess, A. M., Graber, S. G., and Sakmar, T. P. (2000) *Biochemistry* **39,** 3734–3744
46. Oprian, D. D., Molday, R. S., Kaufman, R. J., and Khorana, H. G. (1987) *Proc. Natl. Acad. Sci. U. S. A.* **84,** 8874–8878

47. Combadiere, C., Ahuja, S. K., Tiffany, H. L., and Murphy, P. M. (1996) *J. Leukocyte Biol.* **60,** 147–152
48. Okada, T., Sugihara, M., Bondar, A. N., Elstner, M., Entel, P., and Buss, V. (2004) *J. Mol. Biol.* **342,** 571–583
49. Huber, T., Botelho, A. V., Beyer, K., and Brown, M. F. (2004) *Biophys. J.* 2078–2100
50. Reeves, P. J., Kim, J. M., and Khorana, H. G. (2002) *Proc. Natl. Acad. Sci. U. S. A.* **99,** 13413–13418
51. Chang, P. V., Prescher, J. A., Hangauer, M. J., and Bertozzi, C. R. (2007) *J. Am. Chem. Soc.* **129,** 8400–8401
52. Rasmussen, S. G., Choi, H. J., Rosenbaum, D. M., Kobilka, T. S., Thian, F. S., Edwards, P. C., Burghammer, M., Ratnala, V. R., Sanishvili, R., Fischetti, R. F., Schertler, G. F., Weis, W. I., and Kobilka, B. K. (2007) *Nature* **450,** 383–387
53. Cherezov, V., Rosenbaum, D. M., Hanson, M. A., Rasmussen, S. G., Thian, F. S., Kobilka, T. S., Choi, H. J., Kuhn, P., Weis, W. I., Kobilka, B. K., and Stevens, R. C. (2007) *Science* **318,** 1258–1265
54. Rosenbaum, D. M., Cherezov, V., Hanson, M. A., Rasmussen, S. G., Thian, F. S., Kobilka, T. S., Choi, H. J., Yao, X. J., Weis, W. I., Stevens, R. C., and Kobilka, B. K. (2007) *Science* **318,** 1266–1273
55. Ban, N., Nissen, P., Hansen, J., Moore, P. B., and Steitz, T. A. (2000) *Science* **289,** 905–920
56. Yusupov, M. M., Yusupova, G. Z., Baucom, A., Lieberman, K., Earnest, T. N., Cate, J. H., and Noller, H. F. (2001) *Science* **292,** 883–896
57. Wimberly, B. T., Brodersen, D. E., Clemons, W. M. J., Morgan-Warren, R. J., Carter, A. P., Vonrhein, C., Hartsch, T., and Ramakrishnan, V. (2000) *Nature* **407,** 327–339
58. Harms, J., Schluenzen, F., Zarivach, R., Bashan, A., Gat, S., Agmon, I., Bartels, H., Franceschi, F., and Yonath, A. (2001) *Cell* **107,** 679–688